Cellulose (2022) 29:4565–4577
https://doi.org/10.1007/s10570-022-04570-1

ORIGINAL RESEARCH

Antibacterial and wound healing properties of cellulose acetate electrospun nanofibers loaded with bioactive glass nanoparticles; in-vivo study

Samar S. Sharaf · Amira M. El-Shafei · Rakia Refaie · Abdullah A. Gibriel · Raghda Abdel-Sattar

Received: 25 October 2021 / Accepted: 29 March 2022 / Published online: 23 April 2022

Abstract Bioactive glasses (BGs) have gained great attention owing to their versatile biological properties. Combining BG nanoparticles (BGNPs) with polymeric nanofibers produced nanocomposites of great performance in various biomedical applications especially in regenerative medicine. In this study, a novel nanocomposite nanofibrous system was developed and optimized from cellulose acetate (CA) electrospun nanofibers containing different concentrations of BGNPs. Morphology, IR and elemental analysis of the prepared electrospun nanofibers were determined using SEM, FT-IR and EDX respectively. Electrical conductivity and viscosity were also studied. Antibacterial properties were then investigated using agar well diffusion method. Moreover, biological wound healing capabilities for the prepared nanofiber dressing were assessed using in-vivo diabetic rat model with induced wounds. The fully characterized CA electrospun uniform nanofiber (100–200 nm) with incorporated BGNPs exhibited broad range of antimicrobial activity against gram negative and positive bacteria. The BGNP loaded CA nanofiber accelerated wound closure efficiently by the 10th day. The remaining wound areas for treated rats were 95.7 ± 1.8, 36.4 ± 3.2, 6.3 ± 1.5 and 0.8 ± 0.9 on 1st, 5th, 10th and 15th days respectively. Therefore, the newly prepared BGNP CA nanocomposite nanofiber could be used as a promising antibacterial and wound healing dressing for rapid and efficient recovery.

Keywords Cellulose acetate · Bioactive glass NPs · Wound healing · Electrospun nanocomposite nanofibers

Introduction

Bioactive glasses (BGs) are surface reactive ceramics biomaterials that are biocompatible and hard. BGs were firstly discovered in 1969 by Hench (1991). They consist mainly of silicon dioxide, calcium oxide and phosphorous. Different forms of BGs can be formulated by varying the percentages of their components (Giannoudis et al. 2005). The classical 45S5 bioactive glass which was invented by Larry Hench is composed of 45% SiO_2, 24.5% Na_2O, 24.5% CaO and 6% P_2O_5. It is the most widely studied glass for biomedical applications (Hench 1998). Silica- and phosphate-based glasses were extensively used as bioactive and biocompatible implants which have the

S. S. Sharaf · A. M. El-Shafei · R. Refaie · R. Abdel-Sattar (✉)
Textile Research Division, National Research Centre, Textile Research and Technology Institute, El-Behouth St. (Former El-Tahrir St.), Dokki, P.O. 12311, Giza, Cairo, Egypt
e-mail: raghdahowait@gmail.com

A. A. Gibriel
Faculty of Pharmacy, Biochemistry and Molecular Biology Division, Pharmacology and Biochemistry Department, The British University in Egypt (BUE), Suez Rd, El Sherouk City, Cairo Governorate 11837, Egypt

ability to generate bone-like apatite layer upon interacting with the host medium and this in turn permits biomaterials interaction especially with mineralized tissue. For this reason, they have been widely implemented in repair and/or replacement of bone architectures (Ahmed et al. 2015; Jones et al. 2007; Neo et al. 1993). Recently, BGs have attracted much interest as novel biocompatible scaffold materials for multiple biomedical applications in tissue engineering, regenerative and therapeutic medicine (De Guevara-Fernández et al. 2003; Knowles 2003).

BG bioactivity is not dependent only on its composition but is also affected by its size and shape as well. BGs have well interconnected pore structure varying in size from nanometers to micrometers. It is crucial to tailor morphology and pore architecture of BGs in order to control and improve textural properties before being used in any biomedical application. In general, BG porosity can be optimized by varying chemical constituents, reagent concentrations, reaction temperature and also through adopting various synthetic and mechanical strategies such as the 3D scaffold structures, electro-spinning, foam replication, sol–gel foaming and/or ice-templating (Fu et al. 2008; Wu et al. 2011).

Owing to the well-known stimulating effect of Boron on bone regeneration, addition of the classical network former of B_2O_3 to the bioactive glass system has also been considered to enhance bioactivity of glass ceramic materials (Saranti et al. 2006). B_2O_3-containing bioactive glasses have then further attracted more attention for their potential role to be used in various biomedical applications owing to their lower chemical durability with rapid and more complete conversion to hydroxyapatite upon immersion in simulated body fluid (Huang et al. 2006).

Nanotechnology and size reduction of biomaterials and fibers into nanoscale form generate nanostructured particles which exhibit novel and remarkable physicochemical properties not present in the bulk form. This change is due to the increase in surface area and the adsorptive capacity of such materials. This also offers the ability to utilize them to reinforce nanopolymeric fibers to generate thin bioactive coatings (Alves et al. 2010; Iqbal and Khera 2015). Nanofibrous materials have also attracted great attention in biomedical fields, tissue engineering, wound healing, tissue regeneration and controlled drug release devices (Cui et al. 2010; Meinel et al. 2012). In addition to the small fiber diameter, the nanofibrous scaffolds ensure high surface area with high porosity and interconnected pores which resemble the morphological structure of the extracellular matrix (Kouhi et al. 2013). This makes nanomaterials ideally suited for various biomedical applications such as bone tissue regeneration and wound healing. The latter is mainly initiated in presence of bacteria namely *Staphylococcus aureus*, *Escherichia coli* and *Pseudomonas aeruginosa* microorganisms which induce a complex series of biochemical processes that could ultimately lead to high mortality rates in developing countries with heavy economic burden (Berthet et al. 2017; Naderi et al. 2018; Unnithan et al. 2014).

Plethora of studies have focused on developing wound dressings nanofibers from several polymers using various techniques (Qu et al. 2019). Recently, electrospinning technique has attracted great attention in preparing ultrafine polymeric nanofibers with better properties owing to higher surface area to volume and also length-to-diameter ratios. This technique depends on the use of electric field within a small capillary with particular voltage to be applied on polymer solutions previously prepared with particular viscosity to be ultimately ejected and deposited as a nonwoven fibrous mat with variable shapes and diameters. Yang et al. (2003) was the first to prepare polyacrylonitrile (PAN) ultrafibers containing silver nanoparticles as antibacterial mat. The electrospun produced mat exhibited stronger antibacterial activity as compared to conventional wound dressings. Since then, several synthetic and natural polymeric nanofibers were prepared via electrospinning for wound healing purposes (Wang and Windbergs 2017). The electrospun nanofiber mats with their nanoscale features, large surface area and porosity resemble the morphological structure of the extracellular matrix. Moreover, they can incorporate nanoparticles and biomolecules of interest for extra added bioactivity (Li et al. 2017; Teixeira et al. 2020). They have also excellent permeability for oxygen which is extremely required for rapid wound healing (Majd et al. 2016).

Cellulose is one of the most well-known naturally abundant polymers that are biodegradable, biocompatible and non-toxic with excellent chemical resistance and thermal stability. It has been extensively used as renewable materials in various biomedical applications such as biosensors, scaffolds, chemosensors, packaging filters and films (Lee et al. 2018).

However, the main disadvantage of cellulose is its inability to dissolve in organic and aqueous solvents and this particularly makes it extremely challenging to prepare cellulose based nanofibers via electrospinning technique. The modified cellulose acetate (CA) derivative is instead soluble in several organic solvents and can be electrospun into films and fibers with complex and intricate architecture which can be functionalized with various biomolecules for various biomedical applications (Ghorani et al. 2019; Hashem et al. 2017; Wang et al. 2020). The CA electrospun dressing has excellent mechanical strength and breathability. Although CA lacks antibacterial activity if used alone, it has a good matrix for incorporating various antimicrobial agents and antibiotics for prevention of microbial growth. For instance, CA nanofibers were used in combination with silver nanoparticles (Kalwar and Shen 2019), vancomycin (Buschle-Diller et al. 2007; Felgueiras et al. 2020), berberine (Samadian et al. 2020), honey bee propolis (Sharaf and El-Naggar 2018), gallic acid (Wutticharoenmongkol et al. 2019) or curcumin (Tsekova et al. 2017) as effective and promising wound healing dressing.

Nanotechnology offers a novel approach for development of nanostructured BGs with higher surface area and improved properties with greater bioactivity and biocompatibility. This applies also for BGs used for coatings on biomedical device or used in particulate form or as fillers in composite materials. For instance, BGs nanoparticles have been widely used as fillers in developing composite nanofibers such as poly(epsilon caprolactone) (PCL) and Poly(glycerol-sebacate) (PGS) polymers for various biomedical applications such as tissue engineering, wound healing and bone remodeling (Liverani et al. 2018; Luginina et al. 2020; Moura et al. 2017). It has been proven that synthetic implants of hydroxyapatite and TiO_2 which mimic the nanostructured features of bones increased bone cell adhesion and proliferation (Palin et al. 2005). In bone tissue engineering, a composite scaffolds of nanostructured polymer/bioactive glass could be used to increase the surface area of the BGs allowing faster ion release and deposition in addition to higher adsorption of protein leading to improved regeneration (Boccaccini et al. 2010). Combining nanostructured materials of both BGs and polymer matrices to form composites improves both mechanical and biological properties of scaffolds and could significantly improve attachment and behavior of osteoblast cells (Rezwan et al. 2006; Yao et al. 2005). This indeed could significantly enhance performance in existing biomedical applications with the possibility of creating novel structures for versatile applications.

In this study and for the first time we investigated the biological activities, antibacterial role, wound healing capabilities and the biomedical wound dressing scaffold/application of fabricated cellulose acetate electrospun nanofiber composite loaded with bioactive glass nanoparticles using in-vitro and in-vivo diabetic rat models.

Methodology

Nanocomposite nanofiber fabrication

Cellulose acetate (CA) (39.7 wt.% acetyl content, average Mn = 50,000 g/mol) and bioactive glass nano powder (Purity ≥ 98%) were purchased from Merck (Darmstadt, Germany). CA solution was prepared by dissolving 12% of CA pellets in mixed solvent system consisting of 1:3 of *N,N*-dimethylacetamide and acetone (DMAC/Ac). Different concentrations of BGs (1–3%), dissolved in the same mixed solvent of CA, were added drop by drop to CA solution until clear and homogenous solutions were obtained. Electrospinning was performed at a feed rate of 0.3 ml/h with 25 kV high DC voltages with a distance of 22 cm. The generated mat was collected on the rotating drum and then dried in a vacuum oven and kept in a desiccator.

Fourier transform infra-red spectroscopy (FT-IR)

FT-IR was carried out using the FTIR instrument model 460 plus Jasco (Micro Analytical Center, Cairo University) to validate the chemical structures of the composite nanofibers. KBr powder was used to mix and press samples under high pressure using a manual pellet maker. The DTGS (Globar) laser source was used to generate various wave lengths (ν) (4000–400 cm^{-1}). The software scanned samples and background 64 scans with high resolution (4 cm^{-1}). In order to obtain clear spectra without interference from moisture or carbon dioxide, 15 min were taken for this purpose.

Morphological characterization

A scanning electron microscope (SEM) was utilized to assess the electro-spun fiber morphology using Quanta 250 FEG (Field emission Gun). Electrospun mat/samples were deposited on Aluminium sheet and were coated in gold layer in sputter coater vacuum machine (S150A Edwards-England) for nearly 200 s in order to generate conductive surface. Gold-coated mats were placed in the sample holder of the SEM chamber. SEM morphology images were taken at 5–10 kV (Verreck et al. 2003). The ImageJ software was implemented to calculate nanofiber diameters for the generated SEM images (https://imagej.nih.gov/ij/download.html).

Viscosity and conductivity

The viscosity of the prepared polymer solutions was determined at room temperature using the rotation viscometer (Brookfield-DVBT). Electrical conductivity for the prepared electrospinning polymer was measured by the Myron L Ultrameter II, Model 6P.

In vitro measurement for antimicrobial activity

The antimicrobial activities of the prepared nanofiber mats were determined using the agar well diffusion method (Oxoid, UK). Antibacterial and antifungal activities were tested in vitro against different microorganisms including gram negative bacteria (*Salmonella tyhimurium* and *Escherichia coli*) and the gram positive (Bacillus cereus, *Bacillus subtilis* and *Staphylococcus aureus*). Briefly, a mixture of autoclaved nutrient agar and broth were dissolved in distilled water (pH 7.2). Then in a laminar flow, the latter was cast into previously autoclaved Petri dishes. Nearly one hundred colony-forming units of bacteria were inoculated on Petri dishes and a fabric sample of 292 cm^2 was planted onto the agar dishes. Petri dishes were incubated for 24 h at 37 °C and examined for inhibition zone formation around placed fabric samples. The prepared fabric mats were cut aseptically into small circles of 6 mm diameter and were then placed on the centre of the Mueller Hinton agar (Oxoid, UK) plates inoculated with one of the specified microbes (one at a time). The plates were then incubated at 37 °C for 24 h and inhibition zones were determined according to AATCC 100 test method (Torlak 2008). A free zone of inhibition around the fabric appears as antimicrobial agent migrates from the fabric onto the agar and diffuses outward. All antimicrobial activity tests were carried out in triplicate to ensure reproducibility.

In vivo measurement for biological and wound healing capability

Eight male Sprague Dawley rats (nearly 100–120 g) were obtained from the animal house facility at the National Research Centre (NRC, Egypt). All experimental procedures for the animal study were conducted in compliance with the international guidelines especially the NIH guide for the care and use of Laboratory animals (NIH Publications No. 8023, revised 1978). They were approved by the animal ethics committee of the NRC. Rats were kept in controlled temperature (22° ± 2 °C) and 12 h photoperiod throughout the study. They were fed standard laboratory diet and water for one week to adapt to laboratory conditions. Each rat was housed in polypropylene cage in standard environmental conditions and fed with standard diet and water on a daily basis.

All rats were injected intraperitoneally with streptozotocin at 40 mg/kg for 5 consecutive days to induce diabetes mellitus. Rats are considered to be diabetic if their levels of blood glucose exceed 16.7 mmol/l for 3 consecutive days. Prior to wound creation, rats were generally anesthetized through intraperitoneal injection of Ketamine and Xylazine mixture. Using a hair clipper, razor and shaving cream, rats back hair was removed and then the skin was disinfected with 70% alcohol. A biopsy puncher of 9 mm diameter was used to obtain uniform wounds with equal depth on the rat dorsal side. Rats were then randomly divided into two groups ($n = 4$ rats to negate for any biological difference if any). Each rat within the two groups has been punched in two sites to create two wounds for minimization of any technical differences. The first rat group was dressed with the un-fabricated fiber meanwhile the second rat group was dressed with the CA electrospun nanofiber with BGNP incorporation. The samples were applied as a wound dressing on the wound site precisely. In order to secure the wound dressing, an elastic adhesive bandage was applied and changed on a daily basis to ensure adequate air exposure. Each rat was kept in separate cages with full access to water and diet. Changes in the wound

diameter were monitored by a digital caliper for each rat over the treatment period (15 days). Successful healing would decrease wound diameter with burn edge contraction. The latter was calculated according to the following equation;

$$\text{Wound area } \% = (Wt/Wi) \times 100 \quad \text{(Powell and Boyce 2009)},$$

where, *Wt* is the wound area at certain time point meanwhile *Wi* is the initial wound at day 0.

Skin irritation test

In order to assess skin irritation effect for the prepared nanofibers, the prepared nanofibers were applied topically on the surface of normal rat with hair cut for 3 days. The following symptoms were clearly observed as a sign for skin irritation; itching, erythema, scaring, edema, escher and blisters.

Statistical analysis

Data was analyzed using SPSS software v-15 (SPSS, USA) and GraphPad Prism software V5 (GraphPad, California, USA). Results were expressed as a mean value with its standard deviation (mean ± SD). At least three replicated were conducted for each experiment set. Statistical analysis was performed with Student's *t*-test and samples were considered significant with P value ≤ 0.05.

Results and discussion

Formation and characterization of cellulose acetate nanofibers containing BG nanoparticles (BGNPs)

After stirring cellulose acetate solution for 2 h, different concentration of BG (SiO_2) nanoparticles (BGNPs) (1–3%) were added drop wise with continuous stirring for another 2 h. Several characterization approaches were implemented to evaluate properties of the BG fabricated CA nanofibers. SEM imaging was performed to determine the surface morphology of the prepared BGNP fabricated CA nanofibers (Fig. 1). SEM images showed that the BGNP fabricated CA nanofibers were uniform, straight with flexible and smooth interconnected porous mats with no beads or any deformation at all. It was also obvious that incorporation of BGNPs had no negative impact on the fabricated CA nanofiber morphology. ImageJ software analysis revealed that the majority (83%) of the 1% BGNP fabricated CA nanofibers had average diameters of 100–300 nm. Nearly 40% of the fabricated nanofiber had average diameter of 100–200 nm. It was also noticed that the major diameter of the fabricated electrospun nanofiber decreased significantly with increased percentage for BGNP incorporation. Increasing BGNP incorporation to 2 and 3% resulted in CA fabricated nanofibers with major diameter (50%) of 100–200 nm (Fig. 1).

EDX spectra and quantitative elemental compositions are shown in Fig. 2. As seen in Fig. 2, the EDX of the prepared CA/BGNP nanofibers with different concentrations of BGNP (1–3%) are characterized by various distinctive peaks for the elements C, Si, O and P. The weight percentages for silicon in CA fabricated nanofibers with 1, 2 and 3% of incorporated BGNPs were found to be 1.56, 2.51 and 7.74% respectively.

Electrospun solution properties and electrospinning processing parameters

It is well known that, morphology, density and diameter of the electrospun nanofibers depend on several parameters such as molecular weight, solution concentration, solution viscosity, electrical conductivity, surface tension, dipole moment and dielectric strength. Moreover, processing parameters such as tip-to-collector distance, electric field strength, flow rate, geometry, needle shape, collector composition, temperature, humidity and air flow are main factors affecting electrospinning and mat formation. In order to achieve desirable morphology and fiber diameter, all those parameters should be perfectly managed. Therefore, the effects of those parameters on nanofibers electrospinning have been widely studied to enhance fiber structures, quality and properties. The processing parameters for the electrospinning process were optimized at a flow rate of 0.3 ml/h using a high DC voltage of 25 kV at a distance of 22 cm and the nanofibers were collected on the rotating drum.

As seen in Table 1, incorporating 1% BGNP to CA nanofiber significantly increased solution viscosity mean from 455 to 857cP with an increase in conductivity mean from 4.9 to 6.59µS/cm. This also resulted in increasing fiber diameter from 50–90 to 200–300 nm. Further increase in percentage of

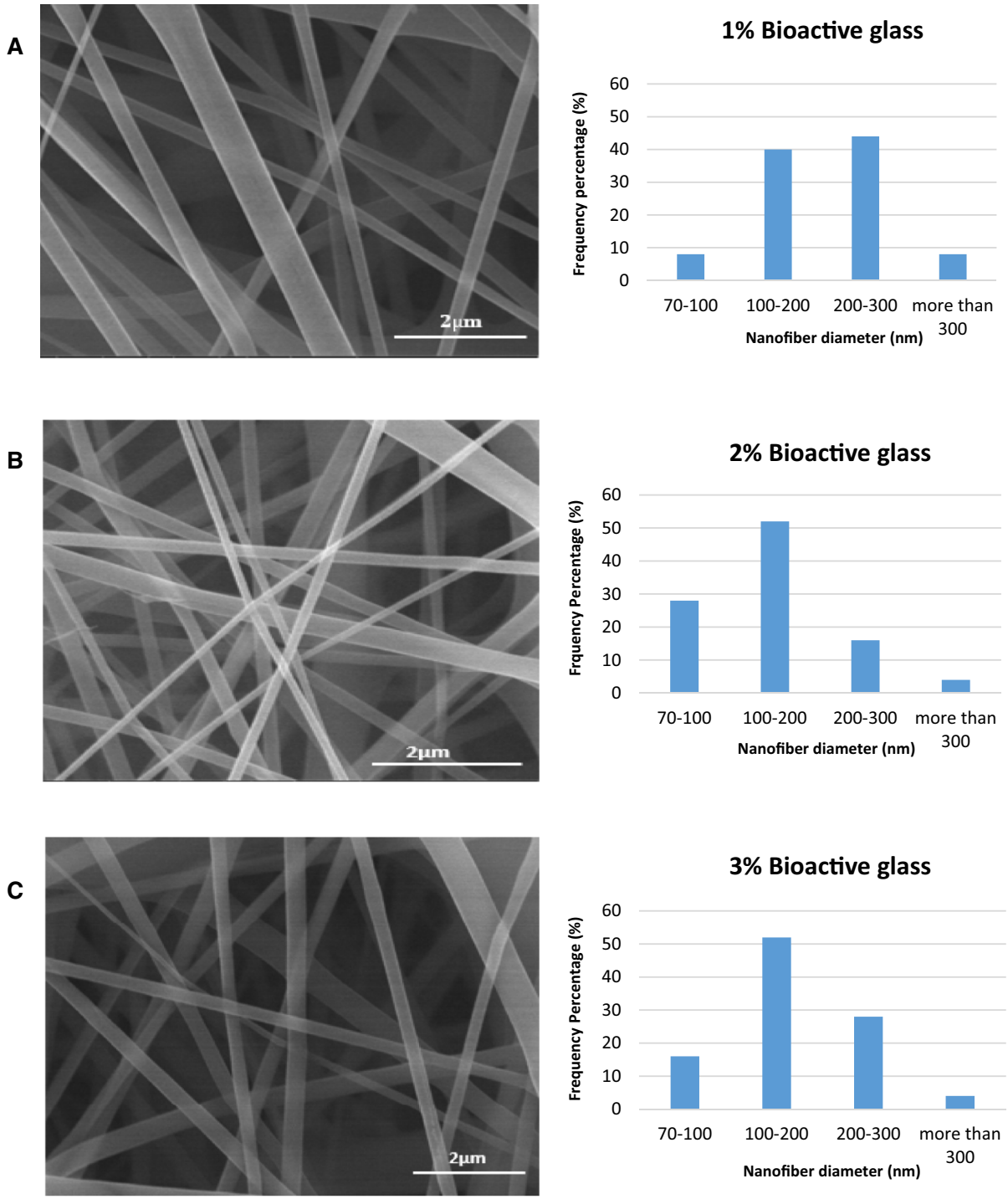

Fig. 1 SEM images and histogram of cellulose acetate nanofibers containing different concentrations of bioactive glass nanoparticles (BGNPs) **a** 1%, **b** 2% and **c** 3%

incorporated BGNPs (2 and 3%) resulted in remarkable decrease in viscosity mean to 585cP and 357cP in 2 and 3% CA incorporated BGNP, respectively (Table 1). There was also significant increase in conductivity mean to 9.68 and 37.7μS/cm in 2 and 3% CA incorporated BGNP, respectively. Increasing percentage of incorporated BGNPs also resulted in reduced fiber diameter range (100–200 nm) (Table1). Such reduction in fiber diameter was also noticed in Fig. 1. This could be attributed to enhanced conductivity and decreased viscosity of the electrospinning solution following incorporation of increasing amount of BGNPs. A possible reason for nanofiber diameter size reduction could be that the incorporation of BG nanoparticles increased the solution charge density which in turn enhanced the self-repulsion of the jet and the stretching forces which led to fiber diameter decrease. Moreover, the presence of BGNP in the fibers increased polymer solution conductivity. The 3% BGNP incorporated CA solution exhibited the highest conductivity and the least viscosity among all prepared solutions with the formation of the most spinnable and finest nanofiber nanocomposite and was therefore selected for further biological and chemical investigations.

FT-IR analysis for the fabricated nanofibers

Fourier transform infrared spectroscopy (FT-IR) was conducted to determine chemical structures of the composite nanofibers. Figure 3 shows the FT-IR spectra for BGNPs (SiO_2), CA and CA containing BGNPs. The FT-IR absorption spectra of glass matrix shows the 2 bands located at 676 and 459 cm^{-1} which correspond to the vibrational mode of the bending of Si–O–B and Si–O–Si (Fig. 3). The 805 cm^{-1} absorption band corresponds to the Si–O symmetric stretch of bridging oxygen atoms between tetrahedrons. The 955 cm^{-1} absorption band which was attributed to the Si–O-bond in (2NBO) was also observed. The band at ~ 1093 cm^{-1} was assigned to the asymmetric stretch vibrations of Si–O bonds in (1NBOS) tetrahedral units. Additionally, two more bands were observed at 1028 cm^{-1} and 560 cm^{-1} where they can be ascribed to the P–O stretching vibration and the P–O bending vibration of amorphous calcium phosphate (ACPs), respectively. The 546 cm^{-1} band is due to the glass structure itself**.** In addition, the 1152 cm^{-1} band was assigned to the P=O stretching vibration (Fig. 3). Moreover, according to Luz and Mano (2011), the existence of bands on 1400–1300 cm^{-1} is related to calcium nitrate precursor due to the N=O bending. The FT-IR spectrum of pure cellulose acetate nanofiber showed three intense peaks at 1373, 1730 and 1222 cm^{-1} which corresponded to the stretching vibration of C–CH3, C=O and C–O–C groups, respectively (Fig. 3). These bands also appear in the FTIR of CA containing BG without presence of any further new peaks. Figure 3 also indicates that there were no chemical reactions occurred in the loading process of nanoparticles.

Antibacterial activity

The antimicrobial effects for the CA and CA/BGNP fabricated nanofiber mats were determined using the in-vitro agar well diffusion method against different bacteria. The prepared nanofibers were incubated for 1 day with the microbial strains on agar plates in order to determine the inhibition zone (halo width). Table 2 shows the reported antimicrobial activity for CA and CA containing BGNP nanofibers. Those results disclose that the BGNP containing CA mat had superior antimicrobial properties as compared to un-fabricated CA mats with wide range of activity against the gram positive (*Bacillus cereus*, *Bacillus subtilis* and *Staphylococcus aureus*) and the gram negative (*Salmonella tyhimurium* and *Escherichia coli*) bacteria. Worth notably, the BGNP containing CA nanofibers were also effective against *Staphylococcus aureus* and *Escherichia coli* strains which represent the most isolated strain from burn and wounds (Berthet et al. 2017; Naderi et al. 2018; Scalise et al. 2015; Unnithan et al. 2014; Zahedi et al. 2010).

It was reported that BGs have antimicrobial activity in aqueous solutions due to the release of their ionic compounds over time. The release of the dissolution products results in high pH environment capable of killing microbes (Waltimo et al. 2007). In addition, the release of silica has been linked to the antibacterial effect of bioactive glass material (Zehnder et al. 2006).

In vivo wound healing experiment

Diabetes mellitus (DM) is one of the major chronic and metabolic disorders which results from uncontrolling blood glucose level. DM is characterized by

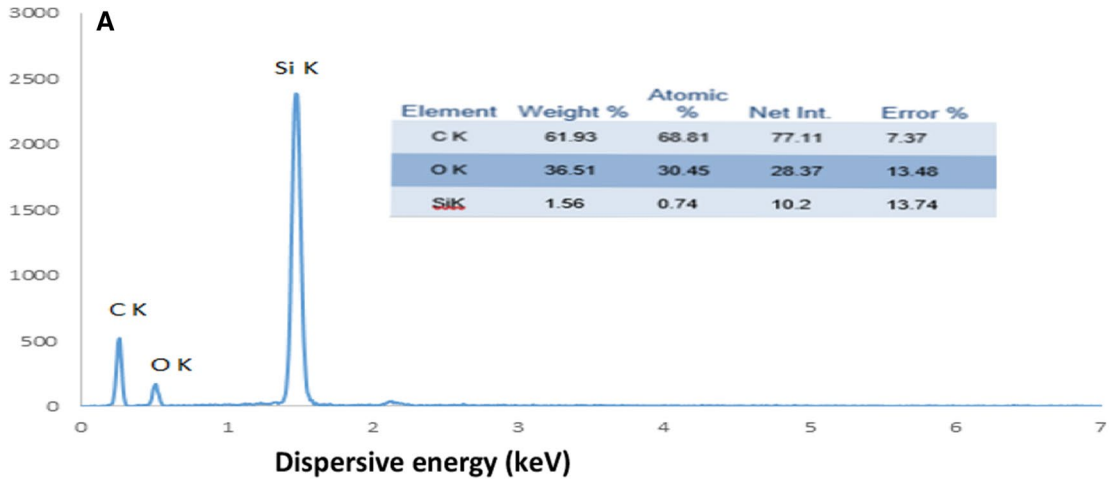
A
Si K
C K
O K
Dispersive energy (keV)
Element Weight % Atomic % Net Int. Error %
C K 61.93 68.81 77.11 7.37
O K 36.51 30.45 28.37 13.48
Si K 1.56 0.74 10.2 13.74

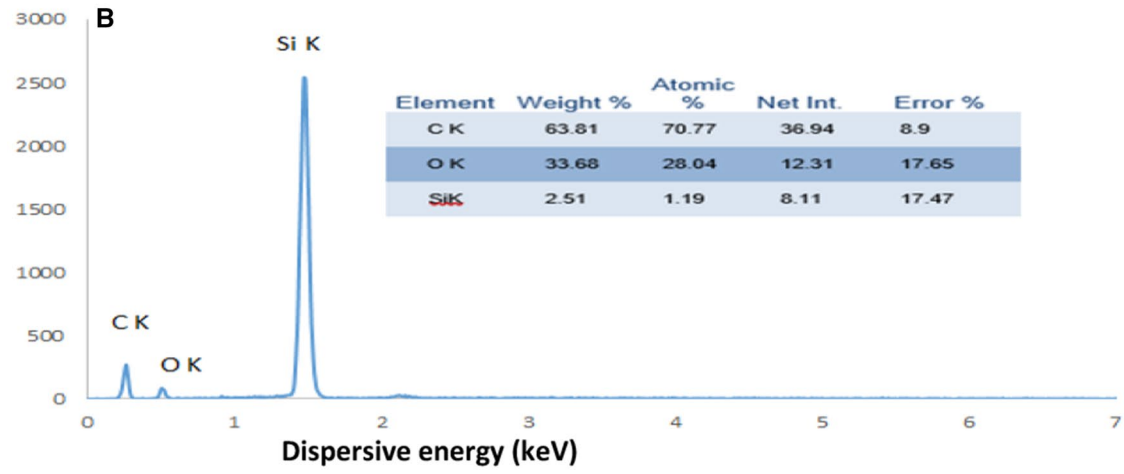
B
Si K
C K
O K
Dispersive energy (keV)
Element Weight % Atomic % Net Int. Error %
C K 63.81 70.77 36.94 8.9
O K 33.68 28.04 12.31 17.65
Si K 2.51 1.19 8.11 17.47

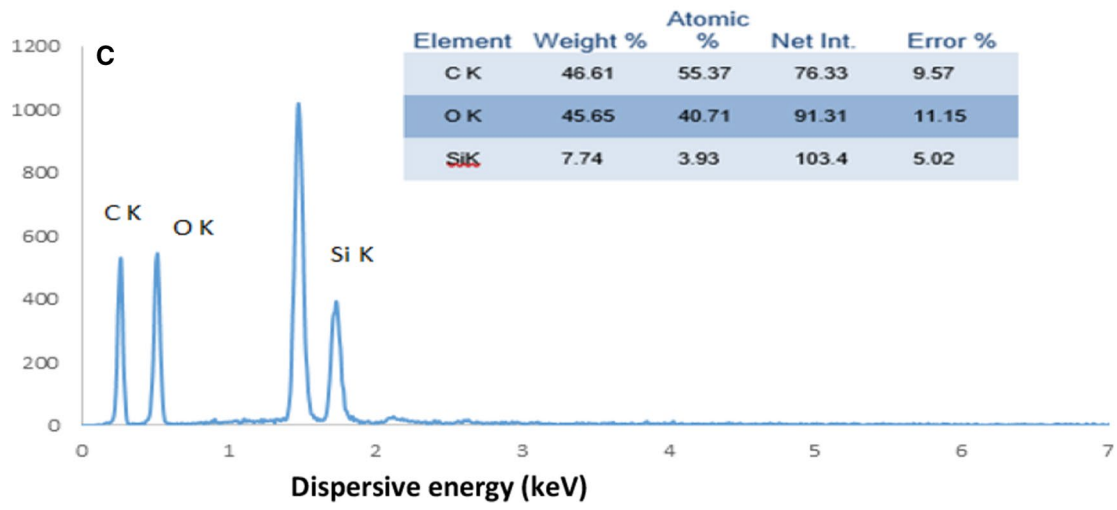
C
C K
O K
Si K
Dispersive energy (keV)
Element Weight % Atomic % Net Int. Error %
C K 46.61 55.37 76.33 9.57
O K 45.65 40.71 91.31 11.15
Si K 7.74 3.93 103.4 5.02

◂**Fig. 2** EDX for of bioactive glass nanoparticles (BGNPs) **a** 1%, **b** 2% and **c** 3%. Cellulose acetate nanofibers containing different concentrations

various complications such as s nephropathy, neuropathy, retinopathy and delayed wound healing efficiency. The latter is a multiphase process which is dependent on blood circulation, angiogenesis and re-epihelialization (Wynn and Freeman 2019). It is also severely affected by inflammation and limited nutrients (Dow et al. 2018). Therefore effective cure for diabetic wounds still remains a great challenge (Jeffcoate et al. 2018).

The most efficient and the most spinnable solution of 3% BGNP incorporated CA was tested for the in-vivo diabetic wound study. All rats recruited in this experiment had very high glucose levels exceeding (16.7 mmol/l equivalent to 300 mg/dl) following intraperitoneal injection of streptozotocin for 3 successive days.

The 9 mm biopsy puncher created uniform wound injuries for each rat with equal depth on the rat dorsal side with no infection, necrosis or exudates on the wound site/area. The firs rat group was dressed with the un-fabricated CA fiber meanwhile the second rat group was dressed with the 3% BGNP incorporated electrospun CA nanofiber. Wound dressing was applied and changed on a daily basis to ensure adequate air exposure. The healing process and wound diameter was monitored over 15 days. Figure 4 illustrates the wound photographs and the healing process on 1st, 5th, 10th and 15th day following wound creation. The diabetic rats which were dressed with the BGNP incorporated electrospun nanofiber initiated the wound healing process from day 1 with significant reduction in wound diameter by day 5 with complete closure by day 10 with uniform adherence to the wound surface with no exudates or necrosis (Fig. 4). By day 15, the wound was completely healed with no marks left. On the other hand, rat group which was treated with the un-fabricated wound dressing did not achieve absolute and efficient wound healing by day 15.

There was significant acceleration for wound healing in the diabetic rats dressed with the BGNP fabricated CA nanofiber as compared to the un-fabricated one. The mean remaining wound areas for the first group treated with BGNP incorporated CA nanofiber were 95.7 ± 1.8, 36.4 ± 3.2, 6.3 ± 1.5 and 0.8 ± 0.9 on 1st, 5th, 10th and 15th days, respectively. It was obvious that the 3% BGNP incorporated CA electrospun nanofiber is a promising wound healing dressing for the prolonged diabetic wound.

Unlike un-fabricated CA nanofibers, the BGNP incorporated CA nanofibers exhibited excellent and efficient wound healing in diabetic rats. This is attributed to the presence of bioactive bioglass. The latter was reported to promote fibroblast proliferative activity and also to accelerate the vascularization process needed for the development and growth of granulation tissue to ensure wound closure and healing. Moreover, the bioactive bioglass was reported to be capable of adsorbing fibroblast, epidermal cells and various growth factors such as vascular endothelial growth factor (VEGF) and fibroblast growth factor-2 (FGF-2) in addition to several other proteins for qucik and efficient cutaneous wound healing (Lin et al. 2012).

Moreover, the prepared BGNP fabricated CA nanofibers that were applied topically on the surface of normal rats for 3 days, following haircut, did not show any signs of erythema, itching, infection, scars, edema, exudates, escher or blisters (Data not shown). This indicates that the prepared nanofibers were safe and does not cause skin irritation to the recruited rats in this study. They were therefore found to be biocompatible with good interaction with fibroblast and skin. Owing to water absorption capability of CA nanofiber, its biocompatibility and its soft interaction with fibroblast cells, CA nanofibers have been considered as excellent wound dressing candidate (Liu et al. 2012).

Conclusion

These newly fabricated CA electrospun nanofiber nanocomposite with incorporated BGNPs were fully characterized in terms of its morphology, IR and elemental composition along with its physical

Table 1 The effects of bioactive glass nanoparticle (BGNP) concentrations on solution viscosity and conductivity along with diameter of the produced nanofibers

Samples	Viscosity (cP)	Conductivity (μS/cm)	Nanofiber produced diameter (nm)
CA	455 ± 23	4.90 ± 0.2	50–90
CA/1%–BG	857 ± 47	6.59 ± 0.4	200–300
CA/2%–BG	585 ± 31	9.68 ± 0.5	100–200
CA/3%–BG	357 ± 14	37.7 ± 1.3	100–200

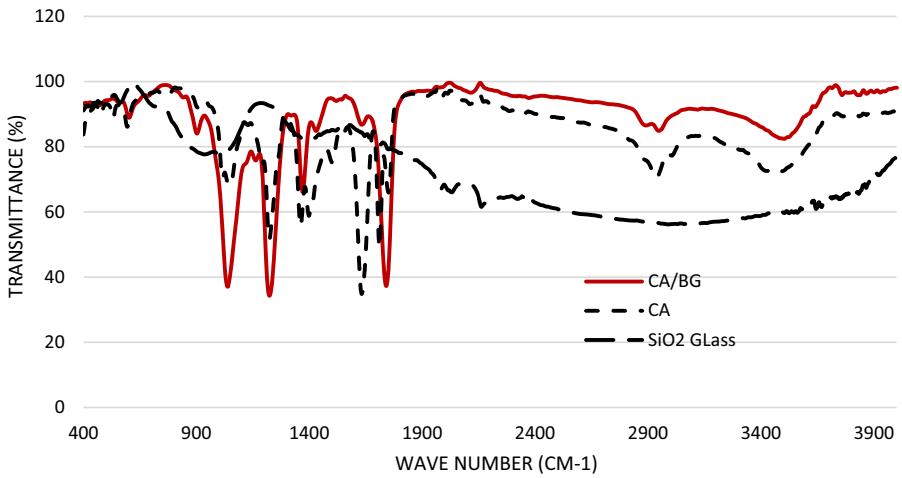

Fig. 3 FT-IR spectra for CA, SiO2 Bioglass (BG) and CA containing BG nanofibers

Table 2 Antimicrobial activity of cellulose acetate (CA) and CA nanofiber containing BG against *Escherichia coli, Salmonella tyhemurum, Bacillus subtilis, Bacillus cereus and Staphylococcus aureus*

Microorganism	Inhibition Zone (mm)	
	CA only	CA containing BG
Escherichia coli 8739	–	34 ± 3.2
Salmonella tyhemurum 14,028	–	31 ± 2.1
Bacillus subtilis 6633	–	29 ± 4.6
Bacillus cereus 33018	–	33 ± 3.4
Staphylococcus aureus 25,923	–	35 ± 2.3

parameters for electrical conductivity and viscosity as well. They demonstrated improved antibacterial activity against wide range of microbes including gram negative and gram positive bacteria with significant reduction of induced wound in diabetic rats with complete healing over limited period. This novel nanocomposite nanofiber could be further applied as a dressing against microbial infection with efficient and rapid wound healing capabilities. Its role in other biomedical applications should be further investigated.

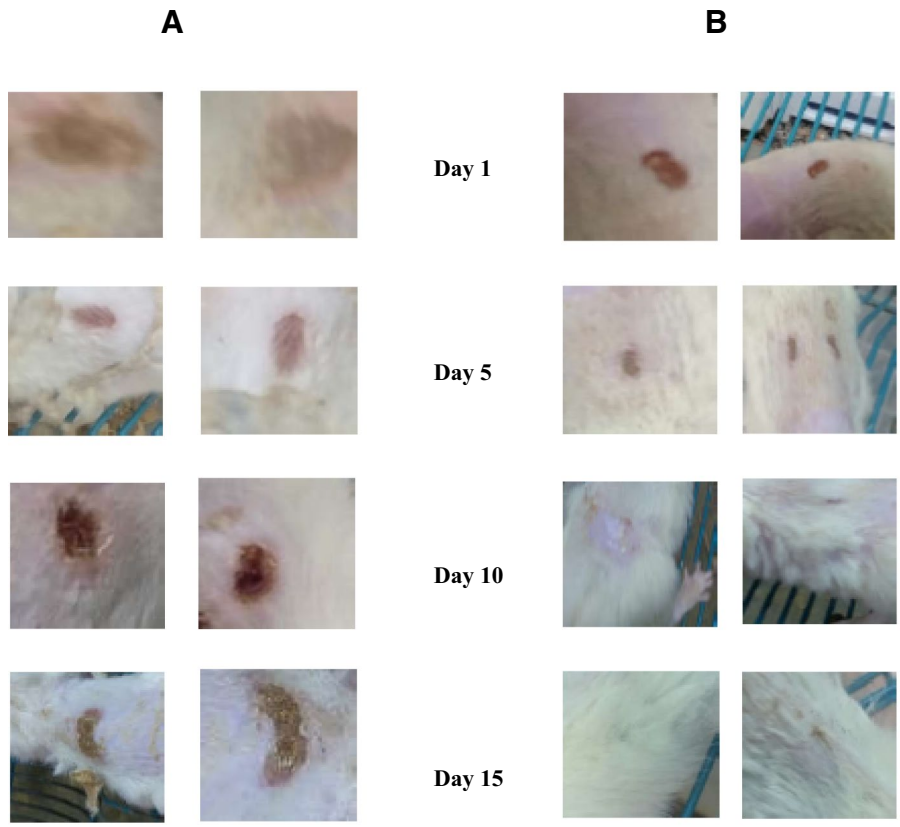

Fig. 4 Effect of **a** unfabricated CA nanofiber and **b** BGNP fabricated CA nanofiber on wound healing process for diabetic rats over a period of 15 days

Funding Open access funding provided by The Science, Technology & Innovation Funding Authority (STDF) in cooperation with The Egyptian Knowledge Bank (EKB). No funding was received to assist with the preparation of this manuscript.

Data availability This article includes all the data generated and analysed during the study.

Declarations

Conflict of interest All authors declare that they have no conflict of interest.

References

Ahmed SA, Gibriel AAY, Abdellatif AK, Ebied HM (2015) Evaluation of food products fortified with oyster shell for the prevention and treatment of osteoporosis. J Food Sci Technol 52:6816–6820

Alves NM, Leonor IB, Azevedo HS, Reis RL, Mano JF (2010) Designing biomaterials based on biomineralization of bone. J Mater Chem 20:2911–2921

Berthet M, Gauthier Y, Lacroix C, Verrier B, Monge C (2017) Nanoparticle-based dressing: the future of wound treatment? Trends Biotechnol 35:770–784

Boccaccini AR, Erol M, Stark WJ, Mohn D, Hong Z, Mano JF (2010) Polymer/bioactive glass nanocomposites for biomedical applications: a review. Compos Sci Technol 70:1764–1776

Buschle-Diller G et al (2007) Release of antibiotics from electrospun bicomponent fibers. Cellulose 14:553–562

Cui W, Zhou Y, Chang J (2010) Electrospun nanofibrous materials for tissue engineering and drug delivery. Sci Technol Adv Mater 1:014108.

De Guevara-Fernández SL, Ragel C, Vallet-Regı M (2003) Bioactive glass-polymer materials for controlled release of ibuprofen. Biomater 24:4037–4043

Dow C, Mancini F, Rajaobelina K, Boutron-Ruault M-C, Balkau B, Bonnet F, Fagherazzi G (2018) Diet and risk of diabetic retinopathy: a systematic review. Eur J Epidemiol 33:141–156

Felgueiras HP, Teixeira MA, Tavares TD, Amorim MTP (2020) New method to produce poly (vinyl alcohol)/cellulose acetate films with improved antibacterial action. Mater Today Proc 31:S269–S272

Fu Q, Rahaman MN, Bal BS, Brown RF, Day DE (2008) Mechanical and in vitro performance of 13–93 bioactive glass scaffolds prepared by a polymer foam replication technique. Acta Biomater 4:1854–1864

Ghorani B, Kadkhodaee R, Rajabzadeh G, Tucker N (2019) Assembly of odour adsorbent nanofilters by incorporating cyclodextrin molecules into electrospun cellulose acetate webs. React Funct Polym 134:121–132

Giannoudis PV, Dinopoulos H, Tsiridis E (2005) Bone substitutes: an update. Injury 36:S20–S27

Hashem MM, Shafei AM, Sharaf SS, Abdel-Sattar R, Mohamed AA (2017) Development and evaluation of novel multifunction hybrid containing cationic softener/TiO2/Herbal oil for cotton based fabrics. Egy J Chem 60:171–183

Hench LL (1991) Bioceramics: from concept to clinic. J Am Ceram Soc 74:1487–1510

Hench LL (1998) Bioceramics. J Am Ceram Soc 81:1705–1727

Huang W, Day DE, Kittiratanapiboon K, Rahaman MN (2006) Kinetics and mechanisms of the conversion of silicate (45S5), borate, and borosilicate glasses to hydroxyapatite in dilute phosphate solutions. J Mater Sci Mater Med 17:583–596

Iqbal M, Khera RA (2015) Nanoscale bioactive glasses and their composites with biocompatible polymers. Chem Int 1:17–34

Jeffcoate WJ, Vileikyte L, Boyko EJ, Armstrong DG, Boulton AJM (2018) Current challenges and opportunities in the prevention and management of diabetic foot ulcers. Diabetes Care 41:645–652

Jones JR, Gentleman E, Polak J (2007) Bioactive glass scaffolds for bone regeneration. Elements 3:393–399

Kalwar K, Shen M (2019) Electrospun cellulose acetate nanofibers and Au@AgNPs for antimicrobial activity—a mini review. Nanotechnol Rev 8:246–257

Knowles JC (2003) Phosphate based glasses for biomedical applications. J Mater Chem 13:2395–2401

Kouhi M, Morshed M, Varshosaz J, Fathi MH (2013) Poly (ε-caprolactone) incorporated bioactive glass nanoparticles and simvastatin nanocomposite nanofibers: preparation, characterization and in vitro drug release for bone regeneration applications. Chem Eng J 228:1057–1065

Lee H, Nishino M, Sohn D, Soon Lee J, Kim I (2018) Control of the morphology of cellulose acetate nanofibers via electrospinning. Cellulose 25:2829–2837

Li H, Williams GR, Wu J, Lv Y, Sun X, Wu H, Zhu L-M (2017) Thermosensitive nanofibers loaded with ciprofloxacin as antibacterial wound dressing materials. Int J Pharm 517:135–147

Lin et al (2012) Healing effect of bioactive glass ointment on full-thickness skin wounds. Biomed Mater 7:045017

Liu X et al (2012) Antimicrobial electrospun nanofibers of cellulose acetate and polyester urethane composite for wound dressing. Jbiomed Mater Res B Appl Biomater 100:1556–1565

Liverani et al (2018) Incorporation of bioactive glass nanoparticles in electrospun PCL/chitosan fibers by using benign solvents. Bioact Mater 3:55–63

Luginina et al (2020) Electrospun PCL/PGS composite fibers incorporating bioactive glass particles for soft tissue engineering applications. Nanomater 10:978

Luz GM, Mano JF (2011) Preparation and characterization of bioactive glass nanoparticles prepared by sol–gel for biomedical applications. Nanotechnol 22:494014

Majd SA, Khorasgani MR, Moshtaghian SJ, Talebi A, Khezri M (2016) Application of Chitosan/PVA Nano fiber as a potential wound dressing for streptozotocin-induced diabetic rats. Int J Biol Macromol 92:1162–1168

Meinel AJ, Germershaus O, Luhmann T, Merkle HP, Meinel L (2012) Electrospun matrices for localized drug delivery: current technologies and selected biomedical applications. Euro J Pharm Biopharm 81:1–13

Moura et al (2017) Development of a bioactive glass-polymer composite for wound healing applications. Mater Sci Eng C 76:224–232

Naderi N, Karponis D, Mosahebi A, Seifalian AM (2018) Nanoparticles in wound healing; from hope to promise, from promise to routine. Front Biosci 23:1038–1059

Neo M, Nakamura T, Ohtsuki C, Kokubo T, Yamamuro T (1993) Apatite formation on three kinds of bioactive material at an early stage in vivo: a comparative study by transmission electron microscopy. Jbiomed Mater Res 27:999–1006

Palin E, Liu H, Webster TJ (2005) Mimicking the nanofeatures of bone increases bone-forming cell adhesion and proliferation. Nanotechnol 16:1828

Powell HM, Boyce ST (2009) Engineered human skin fabricated using electrospun collagen PCL blends: morphogenesis and mechanical properties. Tissue Eng Part A 15:2177–2187

Qu J, Zhao X, Liang Y, Xu Y, Ma PX, Guo B (2019) Degradable conductive injectable hydrogels as novel antibacterial, anti-oxidant wound dressings for wound healing. Chem Eng J 362:548–560

Rezwan K, Chen QZ, Blaker JJ, Boccaccini AR (2006) Biodegradable and bioactive porous polymer/inorganic composite scaffolds for bone tissue engineering. Biomater 27:3413–3431

Samadian H et al (2020) Electrospun cellulose acetate/gelatin nanofibrous wound dressing containing berberine for diabetic foot ulcer healing: *in vitro* and *in vivo* studies. Sci Rep 10:8312

Saranti A, Koutselas I, Karakassides MA (2006) Bioactive glasses in the system CaO–B2O3 P2O5: preparation, structural study and in vitro evaluation. J Non Cryst Solids 352:390–398

Scalise A et al (2015) Microenvironment and microbiology of skin wounds: the role of bacterial biofilms and related

factors. In: Seminars in vascular surgery, 2015. vol 3–4. Elsevier, Amsterdam, pp 151–159
Sharaf S, El-Naggar ME (2018) Eco-friendly technology for preparation, characterization and promotion of honey bee propolis extract loaded cellulose acetate nanofibers in medical domains. Cellulose 25:5195–5204
Teixeira MA, Amorim MTP, Felgueiras HP (2020) Poly (vinyl alcohol)-based nanofibrous electrospun scaffolds for tissue engineering applications. Polym 12:7
Torlak E (2008) Measurement uncertainty in testing for antimicrobial activity on textile materials Accredit. Qual Assur 13:563–566
Tsekova PB, Spasova MG, Manolova NE, Markova ND, Rashkov IB (2017) Electrospun curcumin-loaded cellulose acetate/polyvinylpyrrolidone fibrous materials with complex architecture and antibacterial activity. Mater Sci Eng C 73:206–214
Unnithan AR, Gnanasekaran G, Sathishkumar Y, Lee YS, Kim CS (2014) Electrospun antibacterial polyurethane–cellulose acetate–zein composite mats for wound dressing. Carb Polym 102:884–892
Verreck G, Chun I, Peeters J, Rosenblatt J, Brewster ME (2003) Preparation and characterization of nanofibers containing amorphous drug dispersions generated by electrostatic spinning. Pharm Res 20:810–817
Waltimo T, Brunner TJ, Vollenweider M, Stark WJ, Zehnder M (2007) Antimicrobial effect of nanometric bioactive glass 45S5. J Dent Res 86:754–757
Wang D, Yue Y, Wang Q, Cheng W, Han G (2020) Preparation of cellulose acetate polyacrylonitrile composite nanofibers by multi-fluid mixing electrospinning method: Morphology, wettability, and mechanical properties. Appl Surf Sci 510:145462
Wang J, Windbergs M (2017) Functional electrospun fibers for the treatment of human skin wounds. Euro J Pharm Biopharm 119:283–299
Wu C, Luo Y, Cuniberti G, Xiao Y, Gelinsky M (2011) Three-dimensional printing of hierarchical and tough mesoporous bioactive glass scaffolds with a controllable pore architecture, excellent mechanical strength and mineralization ability. Acta Biomater 7:2644–2650
Wutticharoenmongkol P, Hannirojram P, Nuthong P (2019) Gallic acid-loaded electrospun cellulose acetate nanofibers as potential wound dressing materials. Polym Adv Technol 30:1135–1147
Wynn M, Freeman S (2019) The efficacy of negative pressure wound therapy for diabetic foot ulcers: a systematised review. J Tissue Viability 28:152–160
Yang QB, Li DM, Hong YL, Li ZY, Wang C, Qiu SL, Wei Y (2003) Preparation and characterization of a PAN nanofibre containing Ag nanoparticles via electrospinning. Elsevier SA, Amsterdam, pp 973
Yao J, Radin S, Leboy PS, Ducheyne P (2005) The effect of bioactive glass content on synthesis and bioactivity of composite poly (lactic-co-glycolic acid)/bioactive glass substrate for tissue engineering. Biomater 26:1935–1943
Zahedi P, Rezaeian I, Ranaei-Siadat SO, Jafari SH, Supaphol P (2010) A review on wound dressings with an emphasis on electrospun nanofibrous polymeric bandages. Polym Advanc Technol 21:77–95
Zehnder M, Waltimo T, Sener B, Söderling E (2006) Dentin enhances the effectiveness of bioactive glass S53P4 against a strain of Enterococcus faecalis. Oral Surg Oral Med Oral Pathol Oral Radiol Endod 101:530–535